Electroluminescence materials ZnS:Cu,Cl and ZnS:Cu,Mn,Cl studied by EXAFS spectroscopy

M. Warkentin, F. Bridges, S. A. Carter, and M. Anderson
Physics Department, University of California, Santa Cruz, California 95064, USA
(Received 6 March 2006; revised manuscript received 28 August 2006; published 1 February 2007)

When a high-frequency ac voltage is applied to ZnS:Cu,Cl and ZnS:Cu,Mn,Cl devices, optical fluorescence, known as ac electroluminescence (EL), is observed; it depends on both the Cu (Mn) and Cl dopants. The local structure of these compounds was studied using the extended x-ray-absorption fine-structure (EXAFS) technique to understand the role of Cu and Mn. Data were taken at the *K* edge of Zn, Cu, and Mn, for powder material and for both new and aged (degraded, low EL) devices. The EXAFS data show that Mn substitutes for Zn in the ZnS lattice, whereas Cu has a different local structure (it cannot be fit well with the ZnS structure). For all the Cu edge data, the first shell of neighbors is best fit using an experimental standard obtained from CuS, suggesting that almost all of the Cu resides in tiny CuS-like clusters. Since these clusters are dominant in both the new and degraded samples and do not change with aging, they likely do not contribute directly to the luminescence. Consequently, our results indicate that a very small fraction of the Cu atoms are EL-active; this is consistent with previous models for which the emission centers involve isolated Cu defects or Cu pairs. Thus, a possible explanation for the rapid degradation of a device is that the isolated Cu ions electrodiffuse to the CuS-like clusters, at which point they no longer produce EL. Based on these results, a low-temperature annealing experiment (200C) was carried out that shows that a degraded device can be nearly completely rejuvenated by heating.

DOI: 10.1103/PhysRevB.75.075301 PACS number(s): 61.10.Ht, 78.55.−m, 42.79.−e

I. INTRODUCTION

Copper-doped ZnS is a prominent thick-film ac electroluminescence (EL) material. When driven with a 100–200 V ac supply in the 0.1–100 KHz range, ZnS:Cu,Cl emits a bright blue-green (455 nm) band; using square-wave excitation, blue-green pulses can be observed even at 1 Hz, but they only occur during switching of the voltage. For other codopings, colors from red to blue can also be obtained. At moderate driving frequencies and voltages (i.e., moderate fields), ZnS:Cu,Cl is the longest-lived ac EL material with lifetimes in the thousands of hours;[1] however, these lifetimes are still insufficient for many applications. In contrast, dc EL devices require very high applied fields to obtain emission. The basic understanding of the EL mechanism in this material is due to Fischer during the 1960s and relies on Cu preferentially precipitating at thin needlelike Cu_xS defects (a well known *p*-type semiconductor), which form during the phase transition from wurtzite to the cubic structure upon cooling.[2,3] Note that Cu is nearly insoluble in ZnS and precipitates form at very low Cu concentrations. Because of these defects, a very high *local* electric field can be induced temporarily when an electric field square wave is applied across 20–30 μm particles; the high, local E-field is assumed to be concentrated at the tips of the Cu_xS defects and injects holes and electrons into the host lattice at opposite ends of each defect (which reduces the local field). The current model is that the injected electrons are then captured by shallow donor site traps at one end of the Cu_xS precipitate while holes are trapped on recombination centers at the opposite end; when the ac voltage changes sign, the internal field is reversed and reverse injection occurs. Then, for example, some of the electrons emitted during the negative half of a cycle recombine with trapped holes (produced during the previous positive half of the cycle) to produce luminescence.

A detailed understanding of the electron and hole trap sites is still not complete,[4] but all models use isolated defects or pair defects including some recent theoretical models.[5,6] Electron trap sites include a halide defect on a S site (Cl_S, Br_S), Al on a Zn site (Al_{Zn}), or sulfur vacancies (V_S),[1,4,7] while the hole sites are assumed to be either isolated Cu on a Zn site (Cu_{Zn}) or a pair site involving an interstitial Cu (Cu_iCu_{Zn}).[4,5,7] To achieve good EL, the material must be codoped with Cu and an electron trap defect. In addition, low Cu concentrations produce poor ac EL yet they have significant photoluminescent peaks that can be excited optically. These peaks occur at the same wavelength (energy) as the electrically excited emission.[4] For such low concentrations <10 ppm, only isolated Cu defects are expected. The combined evidence is that for ac EL, the emission occurs when electrons and holes from isolated trap sites recombine after electrical excitation—the Cu_xS-precipitates are required for electron/hole injection into the ZnS host.[1] More recently, ac EL has also been observed in nanoparticles, but might have a different excitation mechanism.[4,8] For more details, the reader is referred to the *Phosphor Handbook*;[1] ac electroluminescence is discussed in Chap. 9, Sec. II.

Part of the evidence for localized emission in the vicinity of precipitates is obtained from optical microscopy. In Fig. 1, we show, using confocal optical microscopy, the emission from several of the small particles (approx 20–30 μm in diameter) used in this study. The emission is not uniform over each particle; instead it emanates from a few bright points, in agreement with the early work of Fischer.[2]

Although the above mechanism for emission is widely accepted, the cause of degradation is poorly understood, and none of the studies have addressed in detail the mechanism for EL degradation. It is known that the device operation lifetime (the time for the ac EL emission intensity to decrease by $1/e$ for a given applied voltage and frequency) is

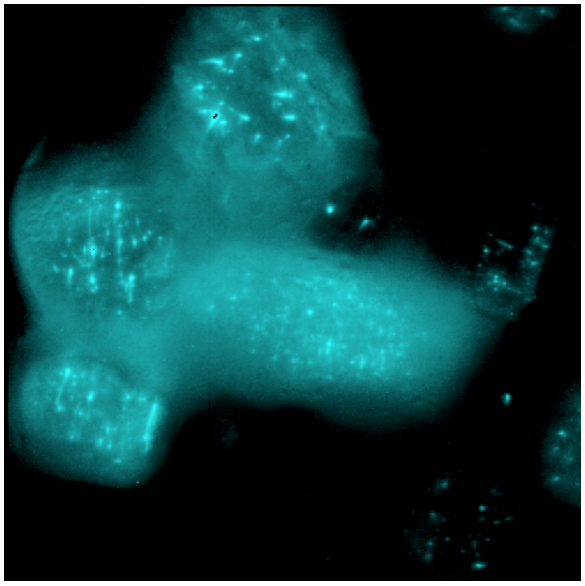

FIG. 1. (Color online) The EL emission from several 20–30-μm-diam particles using a confocal microscope. Note that the emission is not uniform but is produced at a few points in each particle. A micro-probe x-ray scan across such particles shows that the Cu concentration is fairly uniform at the 4 μm level.

dependent on the particle size, but the actual degradation mechanism is not known. Since it must depend on particular details about the emission process—the location of hole and electron trap sites, for example, and whether they can change with time—a better understanding of the degradation process may modify our understanding of the emission mechanism.

An important issue is the nature of the Cu-precipitate—is it like CuS or Cu_2S? In 1990, Ono *et al.* proposed that the Cu_xS phase may actually be Cu_2S (Ref. 9) based on x-ray-absorption near-edge spectroscopy (XANES), and that identification continues to present day.[10] We shall show, however, that XANES is not a good probe of the structure—the edges for CuS and Cu_2S are at essentially the same energy, and extended x-ray-absorption fine structure (EXAFS) is needed to differentiate the two structures.

Thus several major unanswered questions remain: why and how do the ac EL devices degrade and what is the structure of the Cu_xS precipitate—is it Cu_2S- or CuS-like and does it change during device degradation? To gain a better understanding of EL, we have investigated the local environments about the Zn, Cu, and Mn atoms in ZnS:Cu,Cl and ZnS:Cu,Mn,Cl both in powdered materials and in pristine and aged EL devices (ZnS:Cu,Cl), using the EXAFS technique. Our results give new structural information about the Cu environments in ZnS—the primary Cu defect structure is unchanged during device degradation, indicating that the Cu precipitates themselves do not electroluminesce. Thus since isolated Cu defects are assumed to be necessary for the emission,[1,4] at least two different types of Cu defects must be present; our EXAFS results indicate that at the first-neighbor level, the majority of the Cu atoms are in optically inactive CuS-like precipitates and not Cu_2S-like precipitates. The optically active center must be very dilute if the emission occurs in only a very few spots on each particle (Fig. 1) and

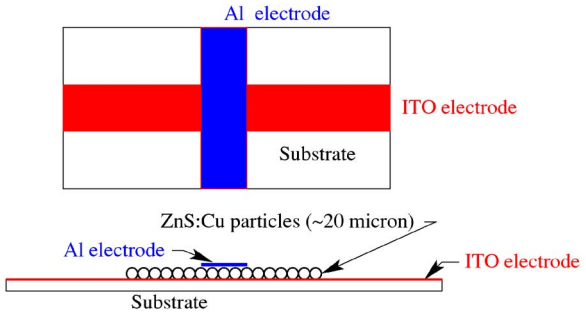

FIG. 2. (Color online) The schematic structure of the EL device used for the EXAFS experiments. The thin plastic substrate allowed transmission EXAFS measurements to be made

there is no observed change in the EXAFS between as made and degraded ZnS:Cu,Cl devices. The EXAFS result therefore supports the proposals that single Cu defects are responsible for the EL emission. Based on these structural results, we propose a model for the degradation mechanism and test this hypothesis through some simple annealing experiments on aged devices. These results shed light on degradation in devices based on Cu-doped ZnS and suggest how the lifetimes might be enhanced.

II. EXPERIMENTAL

Zn, Cu, and Mn *K*-edge EXAFS data were collected on beamlines 4-3 and 10-2 in transmission mode (Zn, Mn, Cu) and also in fluorescence mode (for the dilute Cu and Mn), using Si(220) monochromator crystals, at the Stanford Synchrotron Radiation Laboratory (SSRL). Several different samples were investigated and data were collected at 20 and 300 K. Fine-powder samples were made as follows. ZnS:Cu,Mn,Cl microencapsulated powder (Dupont) was ground in a mortar and pestle and passed through a 400 mesh sieve. The fine powder was then spread onto Scotch tape with a brush—the resulting particle size on the tape was <10 μm. Two layers of tape were pressed together resulting in a double layer; two double layers were used as an EXAFS sample. A similar sample was prepared for ZnS:Cu,Cl. To investigate the effects of device degradation, an EL device was built using the microencapsulated ZnS:Cu,Cl powder ($\sim$20 μm particles), with ITO coated plastic and evaporated Al serving as the two electrodes. A schematic structure is shown in Fig. 2.

For the series of measurements on thin EL devices, Zn and Cu *K*-edge data were first collected on the as-made device, the device was then run at high intensity overnight,[11] and then Zn and Cu *K*-edge data were retaken. A similar device was built using microencapsulated ZnS:Cu,Mn,Cl powder (Dupont), on which Zn, Cu, and Mn *K*-edge data were collected in a similar manner for the as-made device. For the Cu *K*-edge, data were also collected on the reference compounds CuS and Cu_2S at the Advanced Photon Source (APS).

The relative concentrations of the metal dopants were obtained from ratios of the transmission-edge step heights on each sample. In the material containing Mn and Cu, the rela-

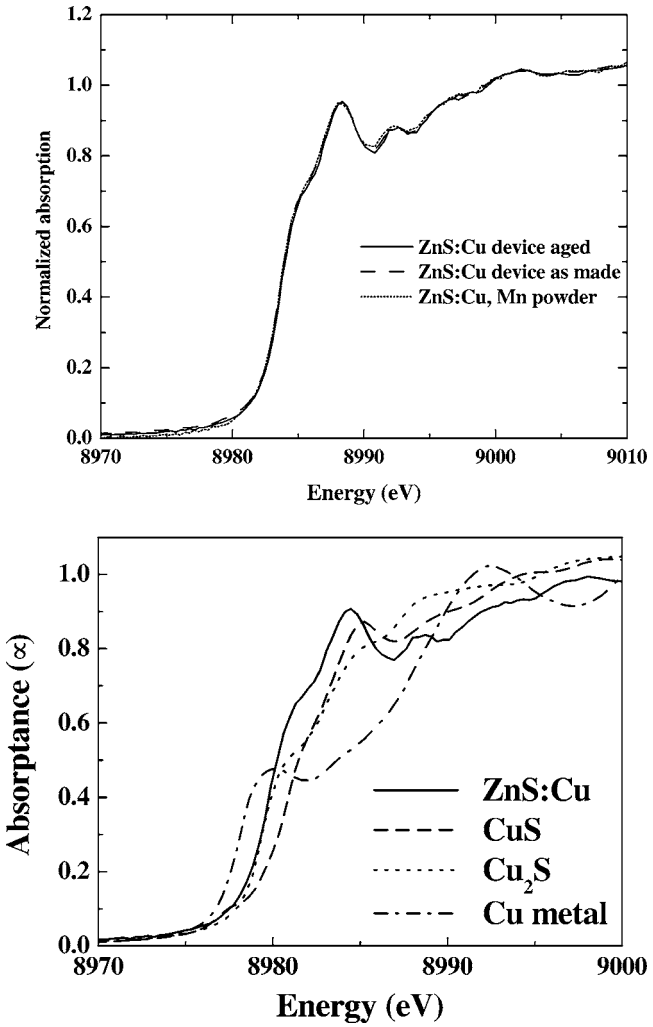

FIG. 3. Top: A comparison of Cu *K*-edge XANES data (20 K) for a ZnS:Cu,Cl device degraded (solid line), a ZnS:Cu,Cl device as made (dashed line), and ZnS:Cu,Mn,Cl powder (dotted line); bottom: XANES for a ZnS:Cu,Cl device (20 K), CuS (30 K), Cu_2S (30 K), and Cu metal (RT). The edge positions have been slightly corrected using a second Cu-metal edge-reference sample at room temperature; the edge-reference data were collected simultaneously with the sample data. All the data are normalized at higher energies: 9100–9200 eV.

tive concentration of Mn is 4.8 at. %, while in both materials, the relative concentration of Cu is ~0.15 at. %.

III. DATA

A. XANES

In Fig. 3 (top), we plot the near-edge structure at the Cu *K*-edge for ZnS:Cu,Cl, as-made and aged devices, and for ZnS:Cu,Mn,Cl material—all at 20 K. There is very little difference between the three traces, indicating that in the XANES there is no change with device degradation and that adding Mn does not change the environment about Cu significantly. Thus the environment about the dominant Cu defect does not change with aging.

In Fig. 3 (bottom), we compare the Cu edge for ZnS:Cu,Cl (20 K) with the corresponding plots for CuS, Cu_2S (both at ~30 K), and Cu metal (RT). Data on a Cu metal reference sample were collected simultaneously to calibrate the monochromator on each beamline. The average edge positions for CuS and Cu_2S are at very nearly the same energy, while that for ZnS:Cu,Cl is slightly lower—also the edge shapes are different. Surprisingly, the average edge position and half-height edge position for the two references and ZnS:Cu,Cl are slightly *below* that of Cu metal. Thus the edge position is not a useful measure of the formal valence in these conducting materials; in particular, the low position of the edge in XANES for ZnS:Cu does not show that the Cu_xS precipitates are Cu_2S as proposed in 1990,[9] because the edge for CuS is also at a comparable energy.

There are many forms of the copper sulfides, Cu_xS_y; Cu_2S and CuS are more common but CuS_2 and $Cu_{2-x}S$ also exist.[12] In addition, several groups consider Cu in both CuS and Cu_2S to behave like Cu^{+1}, with S-S covalent bonds forming S_2^{-1} molecular ions[12,13] for part of the CuS structure. Van der Laan *et al.*[12] describe CuS as a mixture of Cu_2S $(Cu^{+1})_2S^{-2}$ and CuS_2 $[Cu^{+1}(S_2)^{-1}]$. On the other hand, Gotsis *et al.*[13] describe CuS as Cu and S ions in a sea of conducting electrons (which makes these materials quite good conductors). Thus a local probe (EXAFS) is needed to investigate the local structure around Cu in more detail.

It should be noted that for metals such as Cu and Mn, there is a rapid rise in the absorption edge at the Fermi level, which passes through the 3*d* electron density of states. Although a 1*s*-3*d* transition on an atom is forbidden, delocalized (3*d*) conduction electrons can form a state with *p*-like symmetry—and hence have a large *K*-edge absorption for *d* states close to the Fermi energy.[14] Compounds exhibiting metallic conduction should show similar behavior—a sharp absorption increase occurs at the Fermi level; for the systems considered here (ZnS:Cu, ZnS:Cu,Mn), this will again occur within the 3*d* density of states. Thus the usual shift of the 1*s*-4*p* transition with valence, expected from studies of more insulating materials, is not observed for such conducting semiconductors. Note that for bulk ZnS:Mn, the Mn edge passes through the Mn metal edge [very similar to the situation for the Cu *K* edges of ZnS:Cu and Cu metal shown in Fig. 3 (bottom)]. More importantly, the ZnS:Mn edge is approximately 3 eV below the position for a +2 edge (MnF_2) as reported by Soo *et al.*[15] Our results for the Mn *K*-edge XANES are similar to Soo *et al.* and also to Lawniczak-Jablonska *et al.* (12% Mn sample),[16] and are not shown. Another example of a conducting sample with little edge-shift is for the Sr *K* edge in $Sr_8Ga_{16}Ge_{30}$—Bentien *et al.*[17] found that the Sr *K* edge is below that expected for Sr^{+2} and close to that of the elemental metal. We have also obtained similar results in EXAFS studies[18] of a large number of conducting skutterudites—the edges in each case were very close to that for the elemental metal edge.

One last comment on transition-metal edges concerns the presence of preedge peaks that are associated with transitions into unfilled, narrow 3*d* states. Such transitions, which would be forbidden for atomiclike states, become weakly allowed via several mechanisms—including hybridization with *p*

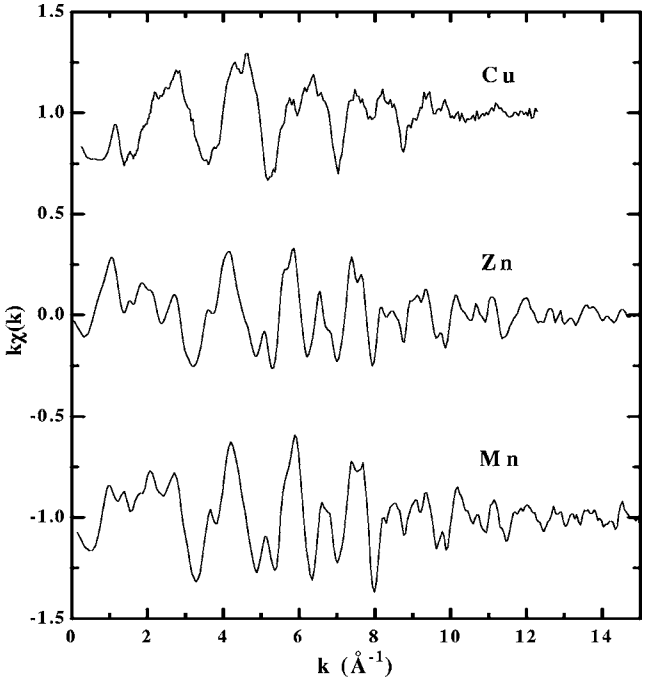

FIG. 4. The *k*-space data obtained from the ZnS:Cu,Mn,Cl fine powder sample at 20 K. The Cu data range is limited by the presence of the Zn *K* edge.

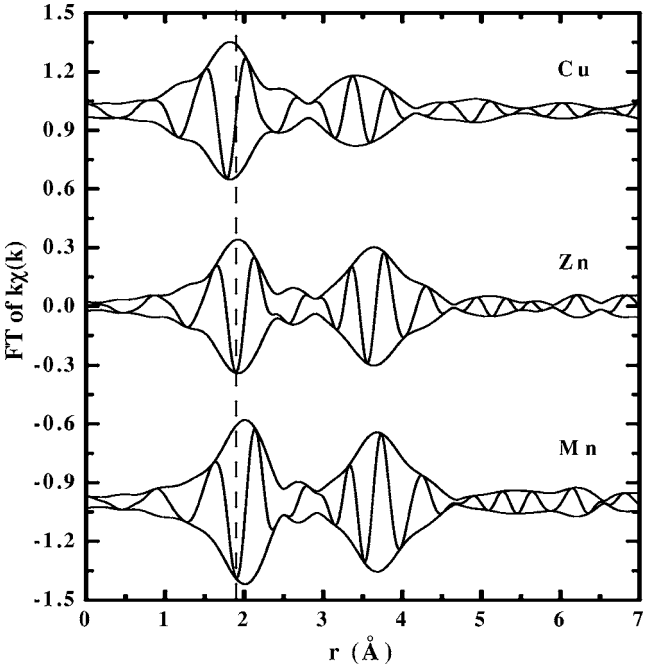

FIG. 5. The *r*-space data obtained from the ZnS:Cu,Mn,Cl fine powder sample at 20 K at the Cu, Zn, and Mn *K* edges. The fast oscillation is the real part (FT_R) of the transform while the envelope is $\pm\sqrt{FT_R^2+FT_I^2}$, where FT_I is the imaginary part of the transform. The vertical line emphasizes the difference in the nearest-neighbor (*S*) positions. For the Cu data, the peak is shifted toward lower *r*, and the phase is shifted as well; in addition, the shoulder from 2 to 2.5 Å is larger for Cu than for Zn or Mn, suggesting a different structure at the nearest-neighbor level. The *k* range for the FTs in this figure was restricted to 4–11 Å^{-1} for comparison with Cu.

states. Such a preedge is oberved in our Mn *K*-edge data as well as in previous reports,[15,16] and indicates some empty *d*-like states just below the main edge. In contrast, the Cu *K* edges in Fig. 3 show no preedge peaks for any of the samples. Since a preedge peak would be expected if Cu were a clear +2 valence ($3d9$ electron configuration; one hole in the $3d$ states), this is further evidence that Cu in ZnS is not Cu^{+2}.

B. EXAFS

The EXAFS data were reduced using standard techniques[19–21] to obtain the oscillatory EXAFS function $k\chi$ as a function of the photoelectron wave vector k. χ is defined in the expression $\mu=\mu_o(1+\chi)$, where μ is the absorption from the edge under study and μ_o is the "embedded atom" background function. Examples of $k\chi(k)$ (called *k*-space data) for the Zn, Cu, and Mn edges are shown in Fig. 4. The Cu and Mn *K*-edge EXAFS required the use of fluorescence mode, due to the low concentrations of those elements in the samples. In addition, data at the Cu edge could only be collected up to 12 Å^{-1} because of the presence of the Zn *K*-edge at 9659 eV near the end of the Cu *K*-edge scan (but up to 15 Å^{-1} for Mn and Zn).

The *k*-space data in Fig. 4 were Fourier-transformed into real space (*r* space) to give the plots shown in Fig. 5. The vertical line is inserted for comparison of the nearest-neighbor peak positions. For neighboring metals in the Periodic Table (here $Z=29$ for Cu and 30 for Zn) and the same type of backscattering atom (here *S*), the central atom phase shift changes slowly with *Z* (Ref. 14); the result is a very small shift of the phase in *r* space. Thus the differences present in Fig. 5 between Cu and Zn indicate a different local structure around Cu—at least a significantly shorter average Cu-S bond; for the range 2–2.5 Å, the data for the Cu and Zn edges are also different. The differences at the second neighbor level (the peak near 3.5 Å) are even larger and likely indicate a changing structure.

In Fig. 6, we compare the *r*-space EXAFS data for a device made using ZnS:Cu,Cl powder, for both the as-made device and the aged device, and a ZnS:Cu,Mn,Cl powder. The data are nearly identical for the two traces for the ZnS:Cu,Cl showing no significant change with aging. The trace for ZnS:Cu,Mn,Cl is very similar—with the most significant difference being a slight change in amplitude for the second neighbor peaks; the difference at low *r* is not significant and depends on the data quality and the background subtraction.

IV. ANALYSIS AND RESULTS

Theoretical EXAFS standards were constructed using FEFF8 (Ref. 22) to fit the *K*-edge data for Zn, Mn, and Cu; the structure (Fig. 7) of pure cubic ZnS (Ref. 23) was used as a starting model. For the Zn *K* edge, we used three single scattering (SS) paths Zn-S (2.342 Å), Zn-Zn (3.825 Å), and a long Zn-S (4.4852 Å). The number of neighbors was fixed at the coordinations for the cubic structure (4, 12, and 12 for

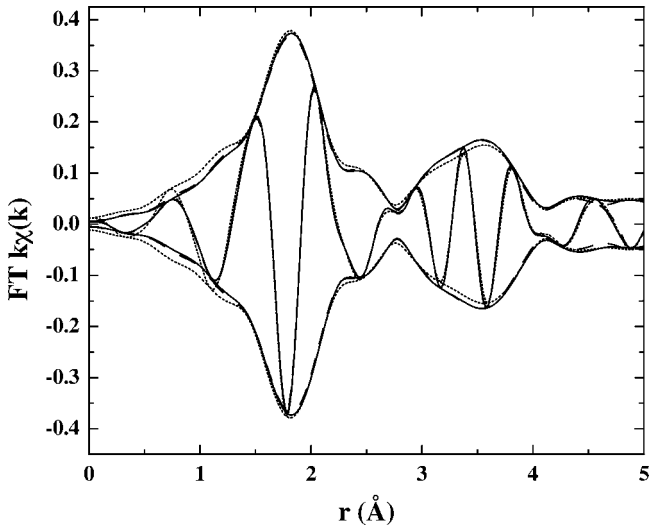

FIG. 6. A comparison of the Cu K-edge EXAFS r-space data [FT $k\chi(k)$] for ZnS:Cu,Cl and ZnS:Cu,Mn,Cl powders at 20 K; solid line, ZnS:Cu,Cl degraded device; dashed line, ZnS:Cu,Cl as-made device; dotted line, ZnS:Cu,Mn,Cl powder. FT range, 3.5–11 $Å^{-1}$.

the first three shells) and the resulting value for $S_o^2 \sim 0.88$ (ranging from 0.85 to 0.9). The pair distances were constrained to the structure—with only one overall distance varied; the first neighbor Zn-S distance in these fits differed by less than 0.005 Å from the starting value from diffraction. The E_o parameter was ~−5 eV. In this fit, we also included two multileg contributions—with distances of 4.255 and 4.685 Å; the latter had a tiny contribution in the fit range and could be excluded. The other multiscattering peak was also small and was constrained to the single scattering peaks. The broadening parameters σ were 0.0585, 0.0625, and 0.696 Å for the three SS paths.

The resulting Zn K-edge fit for ZnS:Cu,Cl (1.6–4.3 Å) is shown in Fig. 8; it fits very well except for a small region between the peaks near 3.0 Å. As described above, the parameters are in excellent agreement with the known structure of ZnS. Some slight extra static disorder and a slightly reduced S_o^2 was observed in the samples containing Mn, but otherwise there was no significant difference in the local structure about Zn between bulk ZnS, the fine-powder sample, or the new and degraded device.

Since the Mn data (Fig. 5) differ from the Zn data by only a small shift in r, it is likely that Mn occupies the Zn sites in the ZnS structure. This suspicion is confirmed by the fit over the first few neighbors (up to 4.3 Å) as shown in Fig. 9. Here we used the same model as used for Zn in Fig. 8, with the core atom replaced by Mn. Again we kept the coordination numbers for the first three shells at the values for ZnS (4, 12, and 12). S_o^2 for the Mn K edge was 0.95±0.05 for several samples. The main difference in the fits was that we allowed the three SS distances to vary independently. The Mn-S bond length increased to 2.41–2.42 Å, slightly longer–by 0.07–0.08 Å–than Zn-S (Note the Mn^{+2} Shannon ionic radius is about 0.06 Å larger than for Zn). In contrast, the Mn-Zn distance increases only 0.03–0.04 Å, while the long Mn-S distance changes very little, 0.01–0.02 Å (estimated

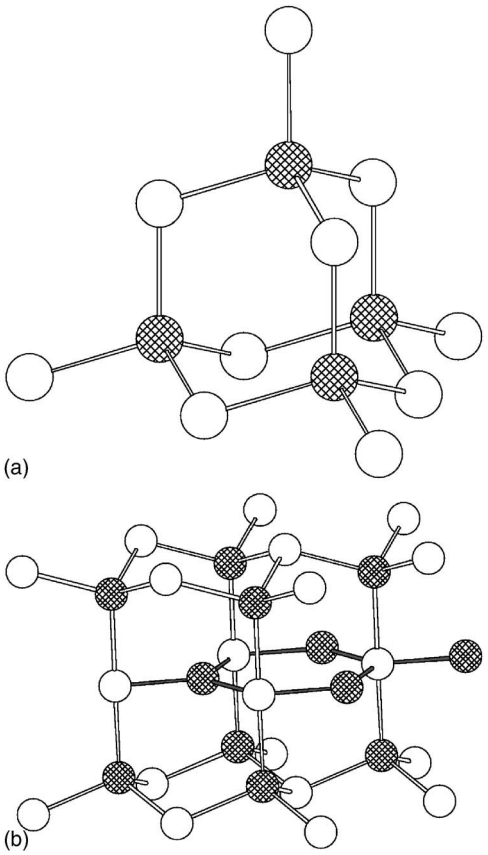

FIG. 7. The structures of ZnS (a) and CuS (b) are depicted. The S atoms are shown as white circles; Zn (a) or Cu (b) atoms are shaded. Note the two distinct Cu sites in the CuS structure (threefold- and fourfold-coordinated).

errors on the distances are ±0.01 Å). This will introduces a small short-range static strain disorder in the ZnS environment. The Mn-S bond length obtained here for $T=20$ K agrees reasonably with the value 2.42 Å reported by Soo *et al.* in Mn-doped bulk ZnS:Mn (no concentration reported) at ~300 K;[15] in that paper, they focused on doped nanoparticles but did report the results for one bulk sample. Our S_o^2 is larger than the value they report (0.81); however, they only had good signal-to-noise up to 8–9 $Å^{-1}$, whereas our data have good signal-to-noise out to ~13–14 $Å^{-1}$.

From Fig. 5, it is apparent that the Cu data are significantly different compared to the Zn and Mn data, which are well fit by the ZnS structure. Attempts were made to fit the first peak in ZnS:Cu,Cl to a contracted ZnS structure with one Cu-S bond length;[24] the quality of the fit parameter was much worse than for the Mn K-edge fluorescence—by an average factor of 8 for ten different traces; in this set of fits, we only used three parameters—σ, r, and amplitude; the same k-space FT range was used for both fits—3.5–11 $Å^{-1}$ (limited by the Cu K-edge data), and the r-space fit range for Mn was 1.7–2.6 Å while that for Cu was 1.6–2.5 Å to include the roughly −0.1 Å shift of the Cu data compared to Mn.

To reduce the number of free parameters and further check the fits, EXAFS data for Cu_2S and CuS were collected at the APS (BM 20), Argonne National Laboratories. The

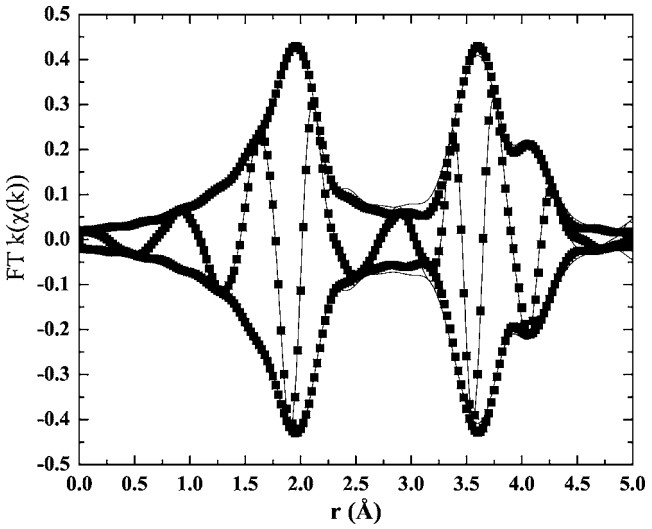

FIG. 8. The fit (squares) to the Zn *r*-space data (lines) at 20 K. The fit includes three two-leg scattering standards (two Zn-S distances, short and long, and Zn-Zn) and two multiscattering standards; the latter were highly constrained. The *r* and *k* ranges over which the fit was performed were 1.6–4.3 Å and 4–14 $Å^{-1}$, respectively (a longer FT range than in Fig. 5).

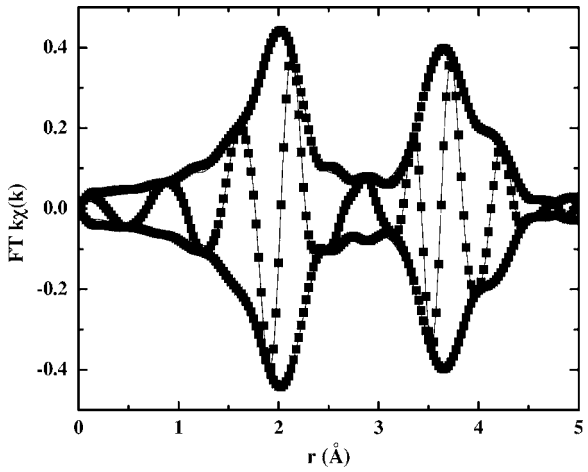

FIG. 9. The fit (solid squares) to the Mn *r*-space data (lines). The fit was similar to the one performed on the Zn data, with the core atom replaced by Mn; the various pair distances were allowed to shift independently. The result is that the nearest-neighbor distance is ~0.07–0.08 Å longer than in the ZnS data. This fit used the same *r* range but a different *k* range compared to the Zn fit—1.6–4.3 Å and 4–12.5 $Å^{-1}$. The values of σ for Mn-S, Mn-Zn, and long Mn-S are 0.053, 0.070, and 0.078 Å, respectively.

r-space data for the Cu_2S sample at 30 K are shown in Fig. 10 (top) and for the CuS sample in Fig. 10 (bottom). For Cu_2S, the shape of the first shell *r*-space peak (1.5–2.5 Å) is different from the corresponding data for ZnS:Cu, particularly the shoulder from 2 to 2.6 Å (see Fig. 5); consequently, Cu in ZnS does not appear to have a local structure similar to Cu_2S. In contrast, the shape of the first peak in the CuS data, especially in the range 2–2.5 Å, appears identical to that for ZnS:Cu (Fig. 5). Note that in the first peak of CuS, there are actually three Cu-S bond distances (2.19, 2.33, and 2.35 Å at 300 K); the Cu_2S structure is more complex.[25]

To quantify the above statements, we used both Cu_2S and CuS as experimental standards to fit the first peak in ZnS:Cu and compared those fits with the fit to a ZnS structure described above. Normally one extracts just the first peak to make such an experimental standard; in this case, we used the entire experimental trace but only fit over the first peak in *r* space. If the local structure is essentially the same as either of these compounds, then the amplitude correction factor $S_o^2=1$ and $\Delta E_0=0$; thus in these fits only two parameters were initially varied—σ and Δr. In Fig. 11(c), we show the poor fit obtained using the Cu_2S standard for the same *r* range 1.6–2.5 Å as described above; the goodness-of-fit parameter is 26.9 times worse than for the fit to the CuS experimental function, and about 12 times worse than the fit using a contracted ZnS structure [Fig. 11(a)]. Thus at the nearest-neighbor level the environment about the majority of Cu is not Cu_2S-like in contrast to the conclusion drawn from the early XANES work.[9]

The best fit is obtained using the CuS standard as shown in Fig. 11(b), again a two-parameter fit over the range 1.6–2.5 Å; note the much better fit over the region 2–2.5 Å. The goodness-of-fit parameter is a factor of 2.1 better for the CuS standard fit than for the fit using a ZnS structure with *four* free parameters. This improvement in the fit increases to a factor of 5.2 if we also allow the amplitude and E_0 to change slightly when using the experimental standard. We also get very similar results for fits to the other two Cu-doped ZnS samples shown in Fig. 6. To quantify the improvement in the fit, we have used Hamilton's F-test for the significance of parameters;[26] the statistical improvement in using the CuS experimental standard for fits using four parameters is ~80%; however, if one fits the data for the three ZnS:Cu samples simultaneously, the statistical improvement using the CuS standard increases to 99%.[27] Thus at the nearest-neighbor level, Cu in both materials (with and without Mn) appears to form tiny CuS-like clusters in ZnS; these clusters contain the majority of the Cu in both new and degraded devices since there is no visible change of the first peak between the as-made and aged devices.

However, the structure for the second- and third-neighbor overlapping shells are quite different for CuS and ZnS:Cu (see Figs. 5 and 10 (bottom)). There is additional weight between 2.3 and 3.3 Å for both ZnS:Cu and CuS compared to the ZnS data. Also, at 4.1 Å there is considerable amplitude for ZnS, but little for either CuS or ZnS:Cu. This difference in the second and third neighbors is consistent with the fact that the shape of the Cu XANES for CuS and ZnS:Cu is also different. Note that the peak in the ZnS:Cu data at 3.4 Å (Fig. 6) is not observed in CuS and is more similar to the peak for ZnS—but with a shift in the peak position to lower *r*. We fit the second-neighbor region for ZnS:Cu (range 3.4–4.2 Å) to a sum of CuS and ZnS experimental traces—the CuS represents the inner part of the cluster while the shifted ZnS simulates a ZnS structure for the ZnS:Cu second neighbors in the interface region. We tried various fits assuming various starting points for the distortion and *r* shift of the ZnS component. The fraction of CuS in such fits is 50±10%. If we assume cylinderlike needle precipitates as suggested by Fischer,[2,3] these results place an

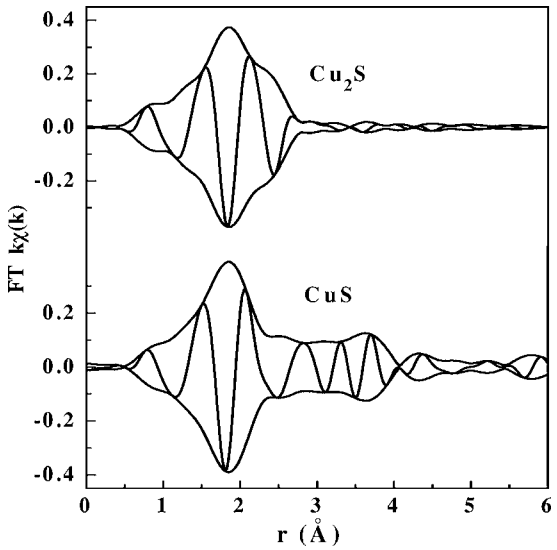

FIG. 10. The *r*-space data for Cu_2S (top) and CuS (bottom) fine-powder reference samples. Based on the shape of the first peak, it is unlikely that a model involving Cu_2S will be able to fit the Cu data from the EL materials. The first peak for CuS looks identical to that for the ZnS:Cu or ZnS:Cu,Mn samples. The FT range for these experimental standards is 3.5–11 $Å^{-1}$.

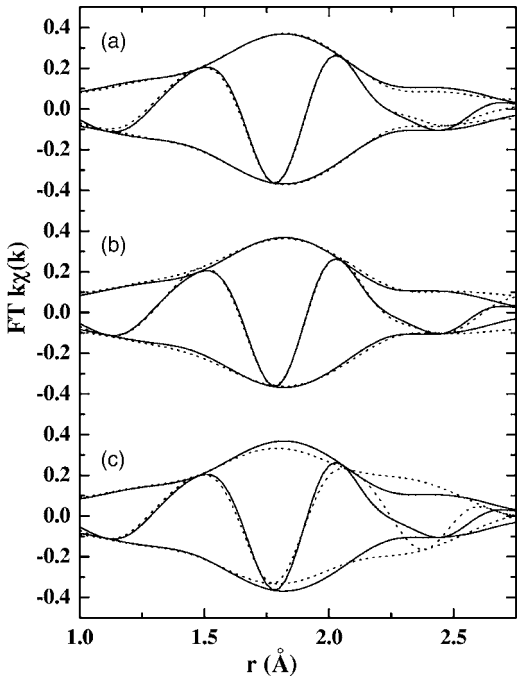

FIG. 11. Fits of the ZnS:Cu data using (a) the ZnS structure (four parameters), (b) the CuS data (two parameters), and (c) the Cu_2S data (two parameters).

upper limit on the cluster diameter of ~1.5 nm; however, no constraints on the length of needlelike nanoprecipitates can be obtained. In addition, there are further neighbors (above 4.5 Å in Fig. 5) observed for ZnS:Cu that are comparable in magnitude to ZnS. Therefore, the CuS-like nanocrystallites are integrated into the ZnS host and do not have a completely random orientation, i.e., there is not an amorphous layer between the CuS-like nanocrystallites and the host crystal.

V. DEGRADATION MODEL AND ADDITIONAL ANNEALING EXPERIMENTS

The results of the Cu EXAFS analysis provide new information about the role of the Cu dopants in producing EL. In a new device, the majority of the Cu atoms reside in small CuS-like clusters or needles with a diameter of order 1–2 nm; these are the clusters reported much earlier by Fischer *et al.*[2,3] Since these clusters remain unchanged after the device has been degraded significantly, it is likely that they are not the EL emission centers. Instead, there must be some other very dilute Cu environment—the recombination centers in the model of Fischer[2,3]—as proposed by Peka *et al.* and Bol *et al.*[5,6] Quite possibly, these centers are substitutional Cu atoms as in the isolated defect model presented by Peka *et al.*,[5] but could be very tiny clusters (pairs), which produces the emission; we refer to these emitting Cu centers as Cu_{EL}. As the device degrades, the concentration of one defect species (for ZnS:Cu,Cl either the Cl or the Cu_{EL} centers) must decrease significantly. Since there is no reported evidence that Cl is clustering while Cu clearly forms precipitates, it is most likely the concentration of Cu recombination centers that decreases. Note that in cooling the sample during preparation, the concentration of isolated Cu defects will be frozen in, and might exceed the small thermal equilibrium concentration expected for a system in which Cu is nearly immiscible, i.e., has large segregation coefficients.[28]

The main mechanism for EL suggests that a high E-field is present near the tips of the Cu_xS needles.[1] This E-field will be transient; it will be largest when the applied voltage is switched, as a combined result of the instantaneous applied field and the previously injected holes and electrons. However, once the charges are redistributed via reinjection, the field will be significantly reduced. During the time the field is high, the diffusion of Cu via hopping will be greatly enhanced. Note that this is consistent with the observation that degradation does not occur with a dc field for the time scales considered here. If an isolated Cu atom reaches the CuS cluster (or perhaps the surface of the 20 μm particles), it likely will remain there and no longer be available for EL.

Evidence for tiny clusters (pairs) comes from the devices made with powder containing both Mn and Cu dopants. The addition of a low Mn concentration changes the emission spectra,[1] which suggests that many of the very dilute, Cu_{EL} emitting centers are close to a Mn atom. Since the Mn-S bond is slightly longer than ZnS while the Cu-S bond is slightly shorter, Mn and Cu may be more stable when they are on adjacent metal sites, as it would reduce the local strains—this has been observed in other systems.[29]

To explore the above degradation hypothesis further, we carried out an annealing experiment on devices based on ZnS:Cu,Cl, and found that for a strongly degraded device, the EL can be rejuvenated by heating at temperatures of only 200 °C. Note that the decomposition temperature of CuS is ~220 °C; it might be even lower for small clusters in a ZnS crystal because of chemical pressure. If the migration of Cu atoms to the clusters is the degradation mechanism, then

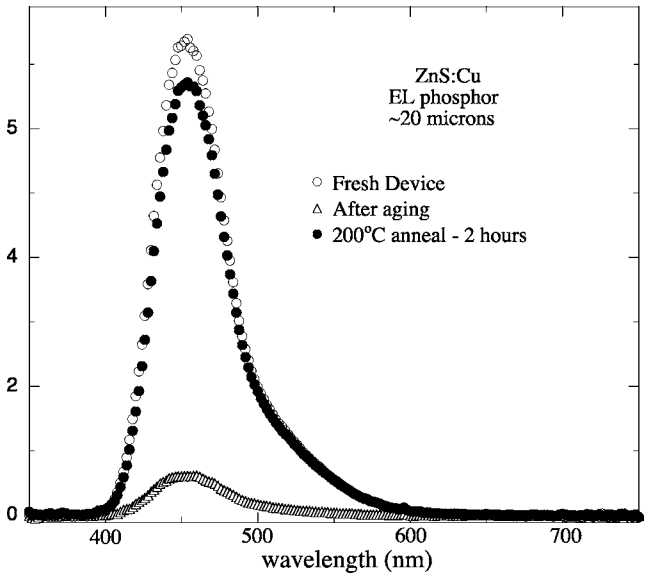

FIG. 12. Electroluminescent intensity as a function of wavelength for an EL device; as made, after aging, and after a subsequent short anneal at 200 °C. After aging, the emission is degraded by a factor of 10; after the short anneal, the emission recovers about 90% of the original intensity.

heating a degraded device sufficiently will allow part of the CuS to dissociate; because of the low decomposition temperature for CuS, heating to a temperature near or above 220 °C should cause some Cu atoms to diffuse away from the CuS clusters, and become EL-active again. This is indeed the case, and nearly complete rejuvenation of ZnS:Cu,Cl based devices after a short anneal (1–2 h) has been observed; this is an important result. In Fig. 12, we plot the emission spectra for a fresh (as-made) device, the spectra for the same device after degradation (operation for several days at 100 kHz) and then after a short anneal at ~200 °C.

These findings provide a clue as to how a longer-lived material might be made. At present Cu concentrations—~0.1%—most of the Cu apparently forms inert CuS-like clusters that produce the high E-fields but not the optical emission. It is likely that these clusters also act as aggregation centers that remove Cu_{EL} from the host matrix. One obvious suggestion is to lower the concentration of Cu in the material by an order of magnitude to slow the formation of the CuS clusters, but that may lower the concentration of Cu_{EL} or reduce the number of CuS-like precipitates too much. Further experiments are clearly needed to determine optimal concentrations and operation conditions (temperature, E-fields, particle size, etc.; also, these parameters may be interrelated) that would lead to longer operation lifetimes.

VI. CONCLUSIONS

In summary, the electroluminescence materials ZnS:Cu,Cl and ZnS:Cu,Mn,Cl have been investigated using the EXAFS technique in order to gain insight into the mechanisms by which these materials emit EL and eventually degrade. No differences in the EXAFS spectra were observed between new and degraded samples; consequently, whatever Cu environment is responsible for the emission, it contains a very small fraction of the Cu atoms even in a new device. The majority environment is that of CuS, but only at the nearest-neighbor level, suggesting that the CuS-like nanoclusters are very small.

The degradation mechanism is quite possibly electrodiffusion of isolated EL-active Cu atoms to the CuS clusters or the particle surface (during field switching); these clusters do not participate directly in the visible emission. Because of the low decomposition temperature for CuS, heating a degraded device to relatively low temperatures (200 °C) can dissociate Cu atoms from the CuS-like clusters and rejuvenate the device, as observed.

ACKNOWLEDGMENTS

We thank C. Booth for the x-ray microprobe data at the Cu *K* edge. Data were collected at SSRL and PNC-CAT at APS. SSRL is operated by the DOE, Division of Chemical Sciences, and by the NIH, Biomedical Resource Technology Program, Division of Research Resources. Research at the PNC-CAT facilities of the Advanced Photon Source (APS) is supported by the U.S. DOE Office of Science Grant No. DEFG03-97ER45628, the University of Washington, a major facilities access grant from NSERC, Simon Fraser University, and the APS. Use of the APS is also supported by the U.S. DOE Offices of Science and Basic Science, Contract No. W-31-109-Eng-38.

[1] S. Tanaka, H. Kobayashi, and H. Sasakura, in *Phosphor Handbook*, edited by S. Shionoya and W. Yen (CRC Press, New York, 1999), Chap. 9, pp. 601–612.
[2] A. G. Fischer, J. Electrochem. Soc. **109**, 1043 (1962).
[3] A. G. Fischer, J. Electrochem. Soc. **110**, 733 (1963).
[4] K. Manzoor, S. R. Vadera, N. Kumar, and T. R. N. Kutty, Mater. Chem. Phys. **82**, 718 (2003).
[5] P. Peka and H.-J. Schulz, Physica B **193**, 57 (1994).
[6] A. A. Bol, J. Ferwerda, J. A. Bergwerff, and A. Meijerink, J. Lumin. **99**, 325 (2002).
[7] R. Revathi and T. R. N. Kutty, J. Mater. Sci. **21**, 2100 (1986).
[8] K. Manzoor, V. Aditya, S. R. Vadera, N. Kumar, and T. R. N. Kutty, Solid State Commun. **135**, 16 (2005).
[9] Y. Ono, N. Shiraga, H. Kadokura, and K. Yamada, J. Inst. Electron., Inf. Commun. Eng. **89**, 378 (1990).
[10] V. V. Bakhmetev, M. M. Sychev, L. Khavanova, V. G. Korsakov, and A. I. Kuznetsov, J. Opt. Technol. **70**, 513 (2003).
[11] The lifetime—the time a device must be run to reduce the intensity to half of its original value—is ~1000 h for ZnS:Cu, Cl when run at 1 KHz. To degrade the device quickly, a 100 V ac source at 100 KHz was applied for 24 h, which is equivalent to one or two lifetimes.

[12] G. van der Laan, R. Parttrick, C. Henderson, and D. Vaughan, J. Phys. Chem. Solids **53**, 1185 (1992).
[13] H. Gotsis, A. Barnes, and P. Strange, J. Phys.: Condens. Matter **4**, 10461 (1992).
[14] B. K. Teo, *EXAFS: Basic Principles and Data Analysis* (Springer-Verlag, New York, 1986).
[15] Y. L. Soo, Z. H. Ming, S. W. Huang, Y. H. Kao, R. N. Bhargava, and D. Gallagher, Phys. Rev. B **50**, 7602 (1994).
[16] K. Lawniczak-Jablonska, R. J. Iwanowski, Z. Golacki, A. Traverse, S. Pizzini, A. Fontaine, I. Winter, and J. Hormes, Phys. Rev. B **53**, 1119 (1996).
[17] A. Bentien, A. E. C. Palmqvist, J. D. Bryan, S. Latturner, G. D. Stucky, L. Furenlid, and B. B. Iversen, Angew. Chem., Int. Ed. **39**, 3613 (2000).
[18] D. Cao, F. Bridges, P. Chesler, S. Bushart, E. D. Bauer, and M. B. Maple, Phys. Rev. B **70**, 094109 (2004).
[19] T. M. Hayes and J. B. Boyce, *Solid State Physics* (Academic, New York, 1982), Vol. 37, p. 173.
[20] G. G. Li, F. Bridges, and C. H. Booth, Phys. Rev. B **52**, 6332 (1995).
[21] See http://lise.lbl.gov/RSXAP.
[22] S. I. Zabinsky, J. J. Rehr, A. Ankudinov, R. C. Albers, and M. J. Eller, Phys. Rev. B **52**, 2995 (1995).
[23] R. W. Wyckoff, *Crystal Structures* (Interscience Publishers, New York, 1960), Vol. 1.
[24] This model would also describe the case in which CuCl nanocrystals form. Both ZnS and CuCl have a zinc-blende structure with lattice constants differing by less than 1%, and S and Cl are comparable scatterers.
[25] R. J. Cava, F. Reidlinger, and B. J. Wuensh, Solid State Ionics **5**, 501 (1981).
[26] W. C. Hamilton, Acta Crystallogr. **18**, 502 (1965).
[27] L. Downward, C. H. Booth, W. W. Lukens, and F. Bridges, *Proceedings of the 13th International Conference on X-ray Absorption Fine Structure-XAFS13* (Stanford, CA, USA, 2006), AIP conference proceedings (2007), to be published.
[28] F. Rosenberger, *Fundamentals of Crystal Growth I*, Springer Series in Solid-State Sciences, Vol. 5, p. 395 (Springer-Verlag, New York, 1979).
[29] F. Rosenberger, *Fundamentals of Crystal Growth I*, Springer Series in Solid-State Sciences, Vol. 5, p. 411 (Springer-Verlag, New York, 1979).